SAE Technical Paper Series

810148

Measurements of Hydrocarbon Concentrations in the Exhaust Products from a Spherical Combustion Bomb

M. C. Sellnau,
G. S. Springer,
and J. C. Keck
Massachusetts Institute of Technology
Cambridge, MA

International Congress and Exposition
Cobo Hall, Detroit, Michigan
February 23-27, 1981

SOCIETY OF AUTOMOTIVE ENGINEERS, INC.
400 COMMONWEALTH DRIVE
WARRENDALE, PENNSYLVANIA 15096

810148

Measurements of Hydrocarbon Concentrations in the Exhaust Products from a Spherical Combustion Bomb

M. C. Sellnau,
G. S. Springer,
and J. C. Keck
Massachusetts Institute of Technology
Cambridge, MA

ABSTRACT

Total hydrocarbon concentrations in the exhaust products from a constant volume heated spherical combustion bomb have been measured using a flame ionization detector. Results were obtained for methane-air and propane-air mixtures as a function of equivalence ratio, initial pressure, wall temperature and inert gas diluent fraction. Although an effort was made to eliminate all crevice volumes and wall contamination, the results indicate that at initial pressures greater than 1 atmosphere, most of the hydrocarbon came from a crevice which was not perfectly sealed. At initial pressures less than 1 atmosphere, it was possible to correct for this and obtain an estimate of the hydrocarbon mass in the quench layer. For an equivalence ratio of unity and no diluent, the hydrocarbon mass per unit wall area was $\leq 0.02\ \mu g/cm^2$. This is only 2% of the value predicted by a theorectical model used to correlate standoff distances on a flat flame burner and suggests virtually complete post-quench oxidation of the quench layer as suggested by Lavoie and co-workers. For nonzero diluent fractions, the wall hydrocarbon concentration increased substantially.

THE REDUCTION OF HYDROCARBON (HC) in the exhaust of automotive engines to comply with Federal regulations is an important problem in automotive engine design. Among the potential sources of such hydrocarbons are (1) quench layers on the cylinder walls [1], (2) crevice volumes into which flames can not propagate [2], (3) oil layers containing absorbed fuel [3] and (4) bulk quenching in the burned gas due to fast expansion [4].

The detailed investigations of these processes in actual engines is difficult due to the complicated geometry and time-dependent turbulent flows involved. For this reason, an investigation of HC in the combustion products of a heated spherical combustion bomb has been made. Similar experiments recently reported by Bergner, et al [5] and Adamczyk, et al [6] have identified crevice volumes as the most important source of HC in bombs. Fast sampling experiments by LoRusso, et al [7] show this is also the case in engines. The present experiments confirm these conclusions, but also show a small contribution from non-crevice sources, most probably an oxidized quench layer as suggested by Adamczyk and Lavoie [8] and Westbrook, et al [9].

EXPERIMENTAL APPARATUS AND PROCEDURE

The spherical combustion bomb used to measure quench layer hydrocarbon concentrations is shown in Fig. 1. The bomb was assembled from

0148-7191/81/0223-0148$02.50

flanged 4150 alloy steel halves and fastened by 12 grade 8 steel bolts. The bomb diameter, interior wall area and volume are 152.4 mm, 765 cm^2 and 1854 cm^3 respectively, corresponding to a surface-to-volume ratio of 0.39 cm^{-1}. Nickel plating on all bomb surfaces provided corrosion resistance and a smooth, glossy surface for flame quenching. A Whitey 1VM4 stainless steel valve, threaded into the bomb wall, was used for charging and exhausting.

Special precautions were taken to seal any crevice volumes that might store unburned fuel. The flange interface, which had the largest crevice volume, was sealed by a thin, soft metal gasket that under compression extruded across the flange (see Fig. 1). All other crevice volumes, including threads and metal-to-metal joints were sealed with SN63 solder (M.P. = 493 K). Initially the two halves of the bomb were joined by 6 bolts and structural flexing of the bomb wall was found to increase the residual hydrocarbon concentration. This effect was eliminated by doubling the number of flange bolts to 12, and thereby doubling the overall bolt stiffness constant. Maximum preload was achieved by using high-strength grade 8 steel bolts and torquing them each to 30,000 psi. Contamination by vacuum grease and RTV sealants was found to contribute to exhaust hydrocarbons and these materials were excluded from use. To minimize contamination from other residual material, the bomb was regularly cleaned with trichloroethylene and rinsed with freon MF solvent.

Bomb heating was provided by a 1.4 kw heated conduction band strapped to the bomb flange. Additionally, a glass wool oven (400 x 400 x 460 mm), fitted with electrical heating coils, enclosed the bomb. An oven fan mounted above the bomb assured temperature uniformity of the oven gases. Four iron-constantan thermocouples distributed within the oven were used to measure temperature. The accuracy of an individual measurement was ±3 K and the bomb temperature was uniform within 10 K.

Two tapered stainless steel electrodes, shown in Fig. 2, projected to the bomb center and served to ignite the fuel-air mixture. The spark gap was varied between 0.020 and 0.045 inches to achieve ignition for a variety of combustible mixtures. A conventional capacitive discharge ignition system with variable voltage and capacitance, served to generate the spark.

During preliminary experiments, it was found that capacitive loading of the high voltage electrode caused surface tracking and spark jumping at the bomb wall. To prevent this and to insure central ignition, the original spark plug insulator was extended by cementing a thin alumina sleeve over the electrode.

Spherically symmetric flames propagated outward from the spark gap and were quenched at the bomb wall. Three ionization probes, two of which were diametrically opposite, were mounted flush with the wall. Flame arrival times were recorded with three high-speed electronic clocks to provide an accurate check of spherical symmetry.

The main features of the apparatus are shown in Fig. 3. The bomb was connected to a 15.3 liter constructed from 316 stainless steel. All connecting plumbing was made of stainless steel, nylon or teflon tubing to preclude catalytic reactions or oxidation in the lines. Neither the storage reservoir nor the connecting plumbing was heated because condensation of either fuel or water was calculated to be negligible.

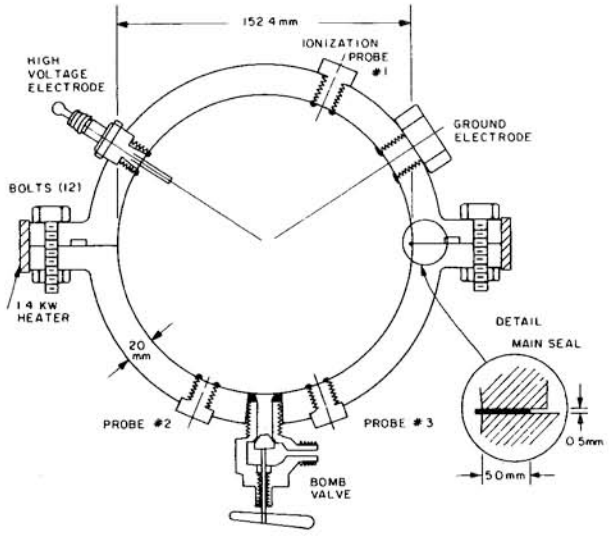

Fig. 1 - Schematic diagram of combustion bomb

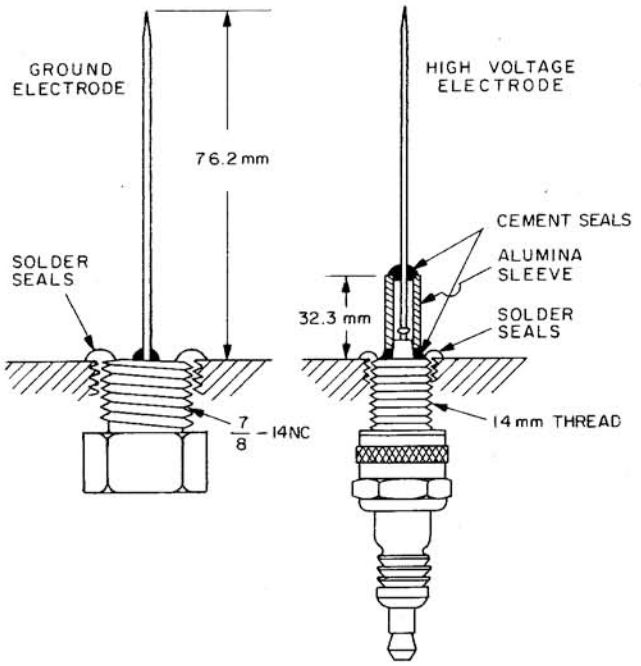

Fig. 2 - Detail of electrodes used for central ignition of the bomb fuel-air mixture charge

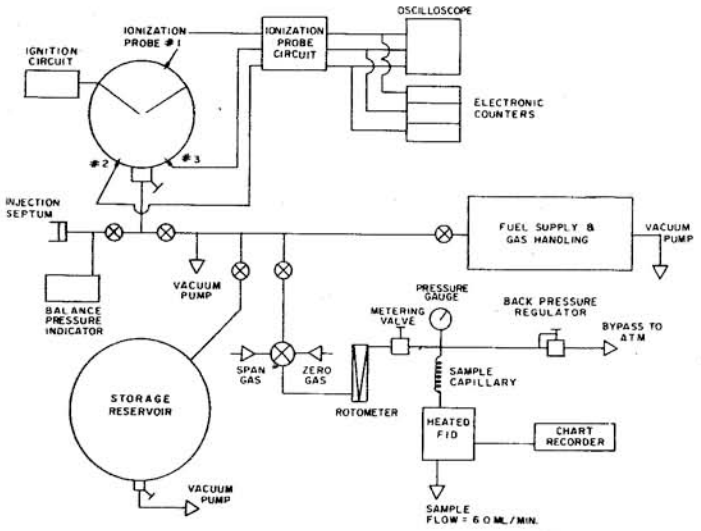

Fig. 3 - Schematic diagram of the apparatus showing gas handling manifold and flame ionization detector

The fuel-air mixture was prepared within the bomb using the method of partial pressures. Initially the bomb was evacuated to 20 to 50 millitorrs. For gaseous fuels, the fuel partial pressure was read directly on a pressure guage (accuracy, .07% FSD). For liquid fuels, an estimated volume of fuel was injected into the bomb and the partial pressure accurately measured utilizing a balance pressure indicator. Finally, air was added until the required total pressure was reached. The propane was Matheson CP grade (99% stated purity); the methane, Matheson technical grade (98% stated purity); and the air was Matheson zero gas.

After charging with reactant gases the bomb contents were allowed to mix for 3 to 5 minutes while the storage reservoir and the connecting plumbing were evacuated. Following ignition and flame propagation, 2 minutes were allowed for cooling and mixing of the bomb gases, after which time, they were blown down to the evacuated storage reservoir. This process cooled the bulk gases and expanded any quench layer on the bomb wall. During this time, gases could also discharge from any unsealed crevice volumes. A jet of nitrogen zero gas (C <0.5ppm) was then simultaneously introduced into the bomb and reservoir, raising the pressure to approximately 2 atmospheres. Finally, after a waiting time of 5 minutes, the well-mixed gases in each vessel were individually sampled by a Perkin-Elmer model F-11 flame ionization detector (FID) and analyzed for total hydrocarbon concentration. The FID was calibrated with propane-N_2 and methane-N_2 mixtures and the output was found to be proportional to carbon atom mole fraction.

A typical strip chart record of the sampling procedure is shown in Fig. 4. Before each test, the FID was calibrated using prepared calibration and zero gases. Hydrocarbon mole fractions in the reservoir and bomb, f_{CR} and f_{CB}, were measured next, with attenuation factors indicated. After measurements, calibration was checked again.

From this record and measurements of the gas pressure and temperature in each vessel, the moles of unburned carbon were computed using the expression

$$N_C = N_B f_{CB} + N_R f_{CR} \qquad (1)$$

where N_B and N_R are the moles of gas in the bomb and reservoir and f_{CB} and f_{CR} are the corresponding measured mole fractions of HC in the sampled gas. Using the ideal gas equation of state

$$pV = NRT \qquad (2)$$

Equation (1) becomes

$$N_C = \frac{P_R}{R}\left(\frac{V_B}{T_B} f_{CB} + \frac{V_R}{T_R} f_{CR}\right) \qquad (3)$$

where T_B and T_R are the temperatures of the bomb and reservoir and P_R is the final pressure in the system after charging with N_2.

The number of moles of products in the bomb after combustion is given by

$$N_b = \left(\frac{W_u}{W_b}\right) N_u = \left(\frac{W_u}{W_b}\right) \frac{P_i V_b}{R T_B} \qquad (4)$$

where W_u / W_b is the molecular weight ratio for unburned and burned gases, N_u is the number of moles of unburned charge initially in the bomb and P_i is the initial pressure. Taking the ratio of Equations (3) and (4), we obtain the mole fraction of carbon in the bomb products

$$f_C = \frac{N_C}{N_b} = \left(\frac{W_b}{W_u}\right) \frac{P_R}{P_i} \left(f_{CB}^* + f_{CR} \frac{V_R T_B}{V_B T_R} \right) \qquad (5)$$

If mixing of the bomb gases were complete prior to blowdown to the reservoir and there were not crevice volumes, f_{CB} should have been equal to f_{CR} . At pressures less than one atmosphere the ratio of f_{CB} / f_{CR} did in fact approach unity. At higher pressure f_{CB} / f_{CR} was found to be an increasing function of pressure indicating both incomplete mixing and crevice volumes. In all cases, however, the major contribution to N_C came from the reservoir due to the large value of the volume ratio V_R / V_B .

As an overall check on the accuracy of the measurement technique, the same procedures were followed with the bomb initially filled with propane-air mixtures having carbon concentrations in the range of those measured for the combustion products. The standard deviation of the measured and known values was less than 2%

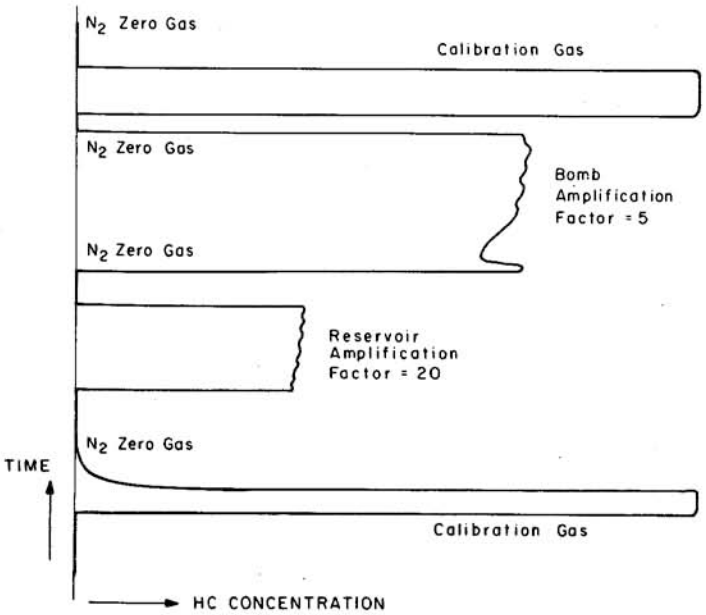

Fig. 4 - Typical strip chart record of the sampling procedure including calibration checkpoints

EXPERIMENTAL RESULTS

Experiments were conducted using propane-air and methane-air mixtures for an initial pressure range of 0.4 to 5.0 atmospheres at wall temperatures of 300, 360 and 410 K. Data at an initial pressure of 1 atm and a wall temperature of 360 K was also collected for a range of equivalence ratios from 0.8 to 1.2 and a range of diluent mass fractions from 0 to 30 percent.

Preliminary measurements with stoichiometric mixtures and no diluent were performed at 1 atm and 300 K while systematically reducing crevice volumes and wall contaminants. Initially, crevices were filled with silicon sealants and vacuum grease. Under these conditions the mole fraction of HC in the bomb products was of the order of 3000 ppmC. Removing these materials reduced the HC levels by a factor of approximately 3. By sealing the crevices with SN63 solder and cleaning the bomb walls with Freon MF solvent, the mole fraction of HC was reduced by another factor of 20 to a value of the order of 20 ppmC

The final results are summarized in Figs. 5 - 7. Fig. 5 shows the HC concentrations, $[N_C] = N_C/V_B$, in the bomb after combustion as a function of the initial unburned charge concentration, $[N_u] = N_u/V_B$. The values have been multiplied by the molar volume of STP, $V_o = 22{,}400\ cm^3$ to make a convenient plot. The results for stoichiometric propane-air mixtures at initial temperatures of 300, 360, and 410 K are shown in the upper part of the figure and the results for methane-air mixtures are shown in the lower part. Note that the mole fraction of HC in the products in ppmC is the ratio of ordinate and the abscissa. It can be seen that the HC concentration increases linearly with initial unburned gas concentration at a rate which is independent of temperature within the accuracy of the data. This strongly suggests that a major fraction of the measured HC came from a crevice volume.

Figure 6 shows the dependence of HC concentrations on fuel-air equivalence ratio, ϕ, for methane-air and propane-air mixtures at an initial pressure of one atmosphere and bomb temperature of 360 K. The results are essentially independent of fuel type and increase roughly linearly with equivalence ratio. This again suggests a crevice volume as the major source of HC.

Fig. 7 shows the dependence of HC concentrations on the mass fraction, f_I, of simu-

lated combustion products added to the unburned gas mixture for propane-air mixtures at an initial pressure of one atmosphere and bomb temperature of 300 K. Combustion products were simulated by diluent mixture of 15% CO_2 and 85% N_2 by volume which was chosen to approximately match the specific heat of real combustion products. It can be seen that the HC concentrations rise rapidly for diluent fractions in excess of 10% by mass. This effect can not be simply explained in terms of HC from crevices and suggests a significant contribution from other sources under these conditions.

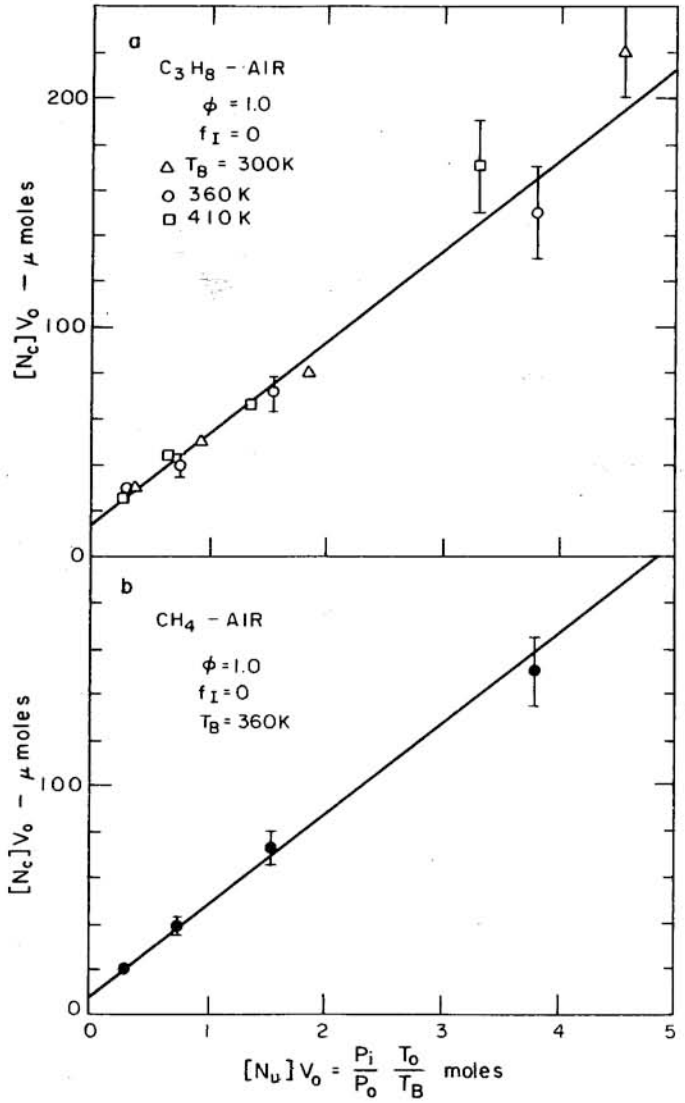

Fig. 5 - HC concentrations $[N_c]$, in the combustion products as a function of initial charge concentration, $[N_u]$ for propane-air (a) and Methane-air (b). The straight lines are least square fits to the data. V_o, P_o, T_o are volume, pressure, and temperature of air at standard conditions

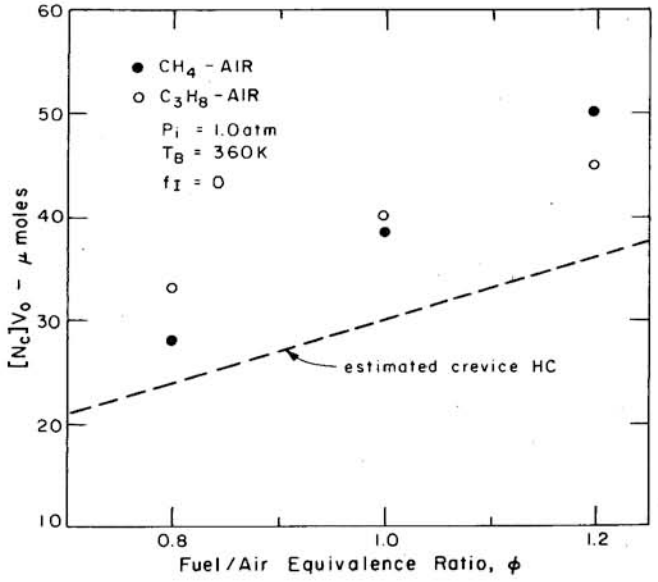

Fig. 6 - HC concentrations $[N_c]$ for propane-air and methane-air as a function of fuel-air equivalence ratio, ϕ. The dashed line is the estimated HC concentration from a 60 mm^3 crevice. Bars represent spread in data

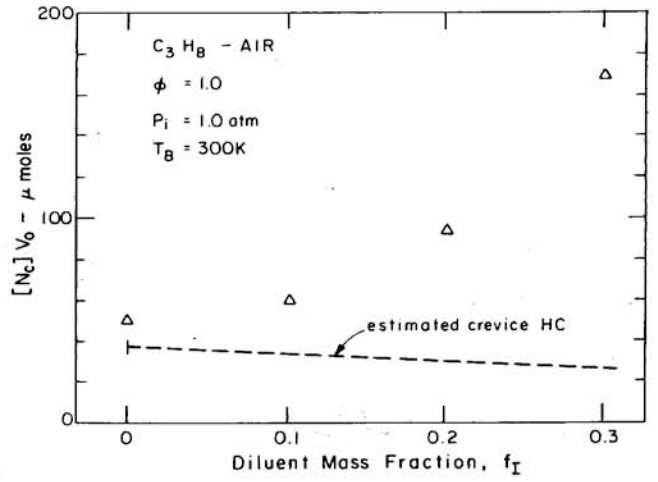

Fig. 7 - HC concentrations $[N_c]$ for propane-air as a function of diluent mass fraction, f_I. The dashed line is the estimated crevice volume concentration

ANALYSIS OF RESULTS

Hydrocarbons from Crevices - The results presented in the previous section strongly suggest a crevice volume as a major source of the HC measured in these experiments. Careful inspection of the bomb after the measurements were completed revealed a crevice in the form of a cylindrical hollow annulus having a volume of

approximately 60 mm^3. The crevice was located behind the ceramic insulator cemented over the high voltage electrode as shown in Fig. 2. The entrance passage to this crevice appears to have been a fine crack in the cement seal created by differential expansion between the metal electrode and ceramic insulator.

Estimates indicate that during the time intervals involved in filling and emptying the bomb, the pressure inside this crevice would equilibrate with that in the bomb. Whether equilibration would occur during the short combustion time of ~40 milliseconds is uncertain. In any case an approximate upper bound to the number of moles of HC stored in crevice following combustion is given by the expression

$$N_{Cc} = f_{Cu} P_p V_c / RT_B \qquad (6)$$

where V_c is the volume of the crevice, P_p is the peak pressure in the bomb at the end of combustion and f_{Cu} is the mole fraction of carbon in the initial mixture.

For a fuel-air mixture containing a diluent fraction f_I and a fuel having the chemical formula $C_n H_m$,

$$f_{Cu} = n\phi(1-f_I) \; / \; (\phi + 4.76\ (n + m/4)) \qquad (7)$$

Dividing Equation 6 by the volume V_B , we obtain the concentration of HC produced by discharge of the crevice into the bomb during cooling of the combustion products,

$$[N_{Cc}] = (f_{Cu} P_p V_c / P_i V_B)\ [N_u] \qquad (8)$$

This equation predicts that, if HC from other sources is negligible compared to that from crevices, the HC concentration in the bomb products should be proportional to the initial unburned gas concentration. This is in good agreement with the data in Fig. 5.

The value of the factor $f_{Cu} V_c P_p / P_i$ obtained from the slopes of the best fit lines in Fig. 5 is 70 mm^3 for both propane and methane. This is very close to the value of 60 mm^3 computed for the electrode crevice volume when charged to the peak pressure and suggests this crevice as the probable source of most of the HC measured.

Non-Crevice Hydrocarbons - It can be seen in Fig. 5, that the intercepts of the best fit lines through the data, though small, are not zero. This fact and the character of the data in Figs. 6 and 7 suggests a possible source of HC in addition to the electrode crevice volume.

Using Equations (7) and (8) and assuming the crevice volume is charged to the final pressure as implied by the data in Fig. 5, one can estimate the contribution of the crevice volume to the HC concentrations plotted in Figs. 6 and 7. These are shown by the dashed lines. Subtracting the crevice contribution from the measured HC concentration gives the HC concentration from non-crevice sources [N_{Cnc}]. These are summarized in the fifth column of Table 1. The sixth column gives the corresponding carbon mass per unit wall area obtained from the equation

$$m_C / A_B = W_C\ [N_{Cnc}]\ V_B / A_B \qquad (9)$$

where $W_C = 12$ is the molecular weight of carbon and A_B is the bomb wall area. The seventh column gives the mass of carbon per unit area obtained from the relation

$$m_{Cq} \; / \; A_B = 3.3\ g_{Cu}\ \lambda_u \; / \; S_u^o\ c_p \qquad (10)$$

derived in the Appendix. In this expression g_{Cu} is the mass fraction of carbon in the unburned mixture, λ_u is the thermal conductivity of the unburned mixture, S_u^o is the adiabatic burning velocity and c_p is the average specific heat at constant pressure for burned and unburned mixture. The laminar burning velocities, S_u^o, measured by Metghalchi and Keck [10] for methane and propane were used in the evaluation of Equation (10). A comparison of the values of m_{Cu}/A_B computed from Equation (10) with those calculated by Westbrook et al. [9] using a detailed chemical kinetic model of flame quenching is shown in Fig. 8. In the range of conditions covered by the detailed calculations, there is good agreement. Equation (10) may also be used to correlate the available data on quenching distances measured for tubes and parallel plates [11].

The last column in Table 1 gives the ratio m_C/m_{Cq}. If indeed the wall quench layer is the source of the non-crevice HC observed, then it is clear from the values of m_C/m_{Cq} that the quench layer has been almost completely oxidized. Virtually complete post-quench oxidation was first predicted by Adamczyk and Lavoie [8] and confirmed by more recent calculations of Westbrook et al. [9]. The fact that m_C/m_{Cq} increases with increasing diluent fraction is consistent with a reduction in the oxidation rate due to the lower temperatures caused by dilution.

A third source of HC which has also been considered is an adsorbed monolayer of fuel on the walls. Assuming a surface concentration of 10^{15} carbon atoms/cm^2, we obtain the value $m_C / A_B \sim 0.02$ ug / cm^2. This could account for the values at zero diluent fraction but is inconsistent with the increase in m_C / A_B with increasing f_I.

Finally there is the possibility of bulk quenching of HC in the combustion products [4]. However, in view of the relatively long residence time of the combustion products in the bomb at high temperatures, the hydrocarbon concentrations in the burned gas should be close to equilibrium and therefore negligible.

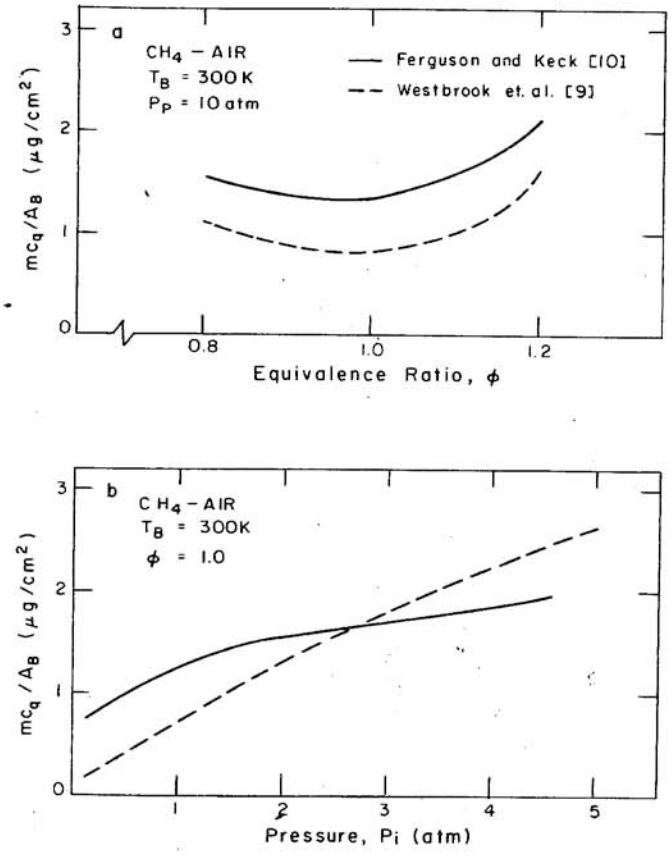

Fig. 8 - Comparison of wall quenched HC calculated by the Ferguson and Keck model [10] and by Westbrook et al. [9] at the moment of quenching

DISCUSSION AND CONCLUSIONS

The HC levels measured in the present experiments are approximately two orders of magnitude lower than the values reported by Agnew for a similar bomb [12]. A comparison with the results reported by Bergner et al. [5] (DFVLR) and Adamczyk et al. [6] (Ford) is shown in Fig. 9. The strong increase of HC with pressure suggests that virtually all the HC measured in the experiments was due to crevice volumes. The departure from linearity in the DFVLR cylinder and Ford sphere data at high pressures is probably due to a distribution of crevice sizes. Since the two-wall quench distance decreases with increasing pressure, thicker crevices tend to burn out more completely at high pressure decreasing the effective crevice volume.

Table 1 - Non-Crevice HC, P_i = 1 atm

Fuel	ϕ	T_B K	f_I	$[N_{Cnc}]V_o$ μ mole	m_C/A_B μg/cm²	m_{Cq}/A_B μg/cm²	m_C/m_{Cq}
CH_4	0.8	360	0	4	.005	.37	.014
CH_4	1.0	360	0	8	.010	.45	.022
CH_4	1.2	360	0	14	.018	.54	.033
C_3H_8	0.8	360	0	9	.012	.53	.023
C_3H_8	1.0	360	0	10	.013	.65	.020
C_3H_8	1.2	360	0	9	.012	.79	.015
C_3H_8	1.0	300	0	12	.016	.81	.020
C_3H_8	1.0	300	.1	25	.032	1.0	.032
C_3H_8	1.0	300	.2	65	.084	1.3	.06
C_3H_8	1.0	300	.3	145	.190	2.3	.08

ϕ = Equivalence ratio
T_B = Bomb wall temperature (K)
f_I = Diluent mass fraction (%)
$[N_{Cnc}]$ = HC concentration from non-crevice sources (μ moles/cm³)
V_o = Molar Volume at STP (cm³)
m_C = Mass of carbon measured in experiments (μg)
m_{Cq} = Mass of carbon calculated from Ferguson and Keck model (μg)
A_B = Area of bomb wall (cm²)

Of the measurements shown, only the M.I.T. data indicate a measurable intercept different from zero, suggesting a possible source of HC other than crevices. This possibility is reinforced by the observation of increasing levels of HC with increasing diluent fraction as shown in Fig. 7.

The most likely source of non-crevice HC is the residue of an incompletely oxidized quench layer. If this were true, the mass of carbon per unit wall area for propane and methane fuel-air mixtures having equivalence ratios between 0.8 and 1.2 would be of the order of 0.02 μg/cm². This is less than 5% of the value predicted for an unoxidized single wall quench layer [11]. In a typical automotive engine, it would produce in-cylinder HC fractions less than 10 ppmC. By comparison, a crevice volume of only 10 mm³, roughly equivalent to the void volume of one turn of the thread on a standard spark plug, would produce 100 ppmC in the cylinder.

For large fractions of exhaust gas recirculation or for non-stoichiometric operation, the quench layer contribution could increase significantly but, until conditions approaching misfire occur, it is unlikely to compete with that from crevices. It is also possible that late combustion followed by rapid expansion could inhibit quench layer oxidation and increase HC from this source in engines. Considering the rapid oxidation rates calculated by Westbrook et al. [9], it is unlikely that the increase would be large except under extreme conditions. On the other hand, the strong turbulence in engines is likely to enhance the oxidation effect producing an even smaller contribution from quench layers than that observed in bombs under laminar conditions.

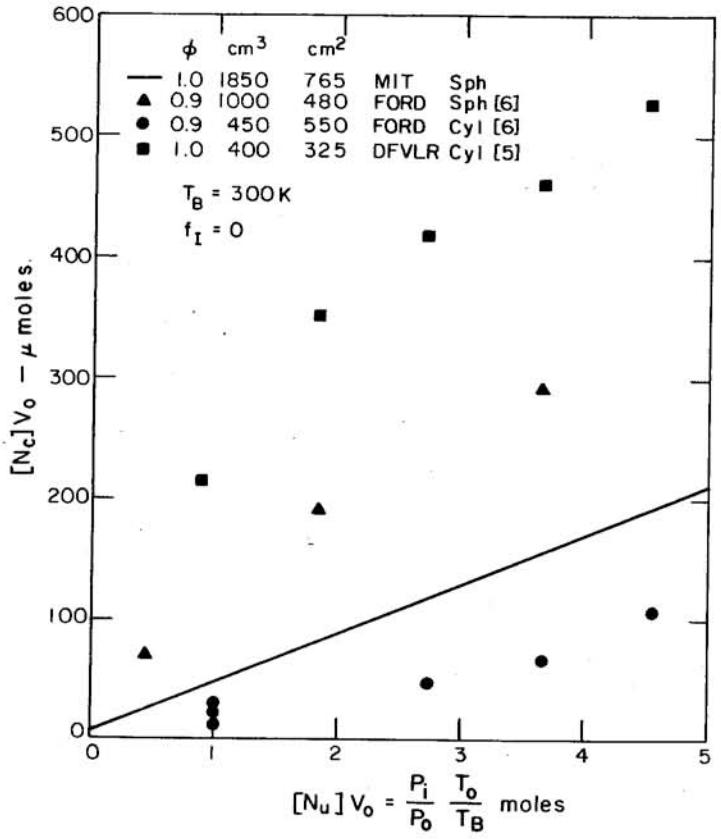

Fig. 9 - Comparison of present measurements (M.I.T. sphere) with those previously reported by Adamczyk et al. [6] (Ford sphere, Ford cylinder) and Bergner et al. [5] (DFVLR cylinder)

In conclusion, it appears from the present measurements and those previously reported by Adamczyk et al. [6] and Bergner et al. [5], that quench layers are a negligible source of HC in engines under practical operating conditions. At the present time, crevice volumes are undoubtedly the major source of both bombs and engines, although bulk quenching or oxidation of oil layers on walls might become important as crevice volumes are reduced or eliminated. These conclusions are supported by the in-cylinder sampling experiments of LoRusso et al. [7] and Weiss and Keck [13] and the theoretical calculations of Westbrook et al. [9].

ACKNOWLEDGEMENT

This work was supported by the Army Research Office under Grant DAAG29-78-C-0010.

REFERENCES

[1] W. A. Daniel, Sixth Symposium (International) on Combustion, The Combustion Institute, 1956.

[2] J. T. Wentworth, SAE Paper 680109, 1968.

[3] E. W. Kaiser, A. A. Adamczyk, and G. A. Lavoie, Eighteenth Symposium (International) on Combustion, Waterloo, Ontario, Canada, August, 1980.

[4] O. I. Smith, C. K. Westbrook, and R. F. Sawyer, The Combustion Institute, Canadian Section, Banff, Alberta, Canada, May, 1977.

[5] P. Bergner, H. Eberino, and H. Pokorny, Third Alcohols Symposium, Asilomar, May, 1979.

[6] A. A. Adamczyk, E. W. Kaiser, J. A. Cavolowsky, and G. A. Lavoie, Eighteenth Symposium (International) on Combustion, Waterloo, Ontario, Canada, August, 1980.

[7] J. A. LoRusso, E. W. Kaiser, and G. A. Lavoie, The Combustion Institute, Eastern Section, Atlanta, November, 1979. Also Paper 800045, SAE Congress, Detroit, February, 1980.

[8] A. A. Adamczyk and G. A. Lavoie, SAE Transactions, 87, SAE Paper 780969, 1978.

[9] C. K. Westbrook, A. A. Adamczyk, and G. A. Lavoie, The Combustion Institute, Western Section, Berkeley, October, 1979.

[10] M. Metghalchi and J. C. Keck, The Combustion Institute, Eastern Section, East Hartford, Conn., November 1977. Also Combustion and Flame, 38, 1980.

[11] C. R. Ferguson and J. C. Keck, Combustion and Flame, 34, 1979.

[12] J. T. Agnew, SAE Paper 670125, 1967.

[13] P. Weiss and J. C. Keck, Paper SAE Congress, Detroit, February 1981.

APPENDIX

LAMINAR FLAME QUENCHING

Following Ferguson and Keck [A1], we assume that the quenching distance, d_q, for a flame propagating toward a cold wall can be approximated by the minimum standoff distance for a flame on a flat burner. To calculate the latter we begin with the equations for steady state one-dimensional flame propagation in the form given by Spalding [A2]

$$\frac{d}{dz}\left(\rho_u S_u C_p T - \lambda \frac{dT}{dz}\right) = \rho_u S_u q \delta(z - d) \quad \text{(A1)}$$

$$\frac{d}{dz}\left(\rho_u S_u g - \rho D \frac{dg}{dz}\right) = -\rho_u S_u g_u \delta(z - d) \quad \text{(A2)}$$

in which the burning rate has been approximated by a delta function $\delta(z - d)$ at the flame position d and where z is the distance from burner, T is the temperature, ρ is the density, C_p is the specific heat at constant pressure, S_u is the flame speed, q is the specific enthalpy of combustion, g is the mass fraction of hydrocarbon, λ is the thermal conductivity, and D is the diffusion coefficient.

In the equation above and those to follow, the subscripts u and b denote conditions in unburned gas at the initial temperature and the burned gas at the final temperature. The appropriate boundary conditions for Equations A1 and A2 are

$$T(\infty) = T_b;\ (dT/dz)_\infty = 0;\ T(0) = T_u \qquad (A3)$$

$$g(\infty) = 0;\ (dg/dz)_\infty = 0 \qquad (A4)$$

If we assume that c_p is a constant and introduce the dimensionless coordinate ξ by means of the transformation

$$d\xi/dz = \rho_u S_u c_p/\lambda \qquad (A5)$$

Equations A1 and A2 can be written in the dimensionless form

$$\frac{d}{d\xi}\left(\tau - \frac{d\tau}{d\xi}\right) = \delta(\xi - P_e) \qquad (A6)$$

$$\frac{d}{d\xi}\left(g - \frac{1}{L}\frac{dy}{d\xi}\right) = -\delta(\xi - P_e) \qquad (A7)$$

where

$$\tau = (T - T_u)/(T_b^\circ - T_u) \qquad (A8)$$

is the dimensionless temperature

$$y = g/g_u \qquad (A9)$$

is the dimensionless mass fraction

$$P_e = \rho_u S_u C_p \int_0^d dz'/\lambda \qquad (A10)$$

is the Peclet number based on d

$$L = \lambda/\rho D c_p \qquad (A11)$$

is the Lewis number and

$$T_b^\circ = T_u + q/c_p \qquad (A12)$$

is the adiabatic flame temperature. The corresponding boundary conditions obtained from Equations A3 and A4 are

$$T(\infty) = \tau_b;\ (d\tau/d\xi)_\infty = 0;\ \tau(0) = 0 \qquad (A13)$$

$$y(\infty) = 0;\ (dy/d\xi)_\infty = 0 \qquad (A14)$$

If we further assume that L is a constant, Equations A6 and A7 can be integrated subject to the boundary conditions of Equations A13 and A14 to give

$$\tau = (1 - \tau_b)(e^\xi - 1) \qquad (A15)$$

$$y = 1 - e^{-L(P_e - \xi)} \qquad (A16)$$

Since $\tau = \tau_b$ at $\xi = P_e$, it follows from Equation A15 that

$$P_e = -\ell n(1 - \tau_b) = \ell n\left(\frac{T_b^\circ - T_u}{T_b^\circ - T_b}\right) \qquad (A17)$$

It also follows that

$$\frac{T}{T_u} = 1 + \left(\frac{T_b^\circ}{T_u} - 1\right) e^{-P_e}(e^\xi - 1) \qquad (A18)$$

Finally if we assume the thermal conductivity can be approximated by

$$\lambda = \lambda_u(T/T_u) \qquad (A19)$$

then Equation A5 can be integrated to give

$$z = \frac{\lambda_u}{\rho_u S_u c_p}\int_0^\xi \frac{T}{T_u}\,d\xi' \qquad (A20)$$

and using Equation A18, we obtain

$$z = \frac{\lambda_u}{\rho_u S_u c_p}\left(\xi + \left(\frac{T_b^\circ}{T_u} - 1\right)e^{-P_e}(e^\xi - 1 - \xi)\right) \qquad (A21)$$

Using Equations A16, A18, and A21, the temperature and concentration profiles can be calculated as functions of z using ξ as a parameter.

Setting $\xi = P_e$ in Equation A21, we obtain the standoff distance

$$d = \frac{\lambda_u}{\rho_u S_u c_p}\left(P_e + \frac{T_b^\circ}{T_u} - 1\right)e^{-P_e}\left(e^{P_e} - 1 - P_e\right)) \qquad (A22)$$

Taken as a function of T_b, this expression has a strong minimum at the point where

$$\partial d/\partial T_b = 0. \qquad (A23)$$

For large values of the Peclet number, Equation A22 can be approximated by

$$d \approx \frac{\lambda_u}{\rho_u S_u C_p}\left(P_e - 1 + \frac{T_b^\circ}{T_u}\right). \qquad (A24)$$

and Equations A23, A24, and A17 lead to the relation

$$\left(\frac{\partial \ell n\, S_u}{\partial T_b}\,(T_b^\circ - T_b)\left(P_e - 1 + \frac{T_b^\circ}{T_u}\right)\right)_q \approx 1 \qquad (A25)$$

where the sbuscript q is used to denote conditions at the minimum standoff distance which we have assumed equal to the quenching distance d_q.

Using the empirical expression [A3]

$$S_u = S_u^\circ \exp\left(-\frac{E_A}{2R}\left(\frac{1}{T_b} - \frac{1}{T_b^\circ}\right)\right) \qquad (A26)$$

where S_u° is the adiabatic flame speed and E_A is an apparent activation energy we find from Equations A25 and A17

$$\frac{E_A}{2RT_b^\circ}\left(1 - \frac{T_u}{T_b^\circ}\right)\left(P_{eq} - 1 + \frac{T_b^\circ}{T_u}\right)e^{-P_{eq}} \approx 1 \qquad (A27)$$

where we have used the approximation $T_b^\circ \approx T_{bq}$ which is valid for $P_{eq} > 1$. The solution of this equation is shown graphically in Fig. A1 in which P_{eq} is plotted as a function of the dimensionless activation energy $E_A/2RT_b^\circ$ for two values of the ratio T_b°/T_u in the range of interest. It can be seen that P_{eq} is a relatively weak function of both $E_A/2RT_b^\circ$ and T_b°/T_u and that for the expected range of $E_A/2RT_b^\circ$ a value of $P_{eq} \approx 4$ is a good approximation.

Substituting Equation A27 back into Equation A26 and again using Equation A17 and assuming $T_b^\circ \approx T_q$

$$S_{uq} \approx S_u^\circ \exp\left(\left(P_{eq} - 1 + \frac{T_b^\circ}{T_u}\right)^{-1}\right) \qquad (A28)$$

which in turn may be substituted into Equation A24 to obtain the quenching distance

$$d_q \approx \frac{\lambda_u}{\rho_u S_u^\circ c_p}\left(P_{eq} - 1 + \frac{T_b^\circ}{T_u}\right) \exp\left(\left(P_{eq} - 1 + \frac{T_b^\circ}{T_u}\right)^{-1}\right) \qquad (A29)$$

The corresponding mass of hydrocarbon quenched per unit area is given by

$$\frac{m_C}{A} = \int_0^{d_q} \rho g\, dx \qquad (A30)$$

Using the equation of state ρT = constant and Equations A5, A9, and A19, Equation A30 can also be written

$$\frac{m_C}{A} = \frac{g_u \lambda_u}{S_u c_p}\int_0^{P_{eq}} y\, d\xi \qquad (A31)$$

Finally substituting Equation A16 into Equation A31 and integrating, we find

$$\frac{\hat{m_C}}{A} \approx \frac{g_u \lambda_u}{S^\circ C_u p}\left(P_{eq} - \frac{1}{L}\left(1 - e^{-LP_{eq}}\right)\right) \qquad (A32)$$

$$\left(\exp\left(\left(P_{eq} - 1 + \frac{T_b^\circ}{T_u}\right)^{-1}\right)\right. \qquad (A33)$$

in which we have used Equation A28.

Dimensionless plots of Equations A31 and (A29) are shown in Figure A1 as a function of E_A 2 RT_b° for L = 1 and several values of T_b°/T_u in the range of interest. Both d_q and m_q/A are insensitive to the values of $E_A/2\ RT_b$ and L, and are well approximated by

$$d_q \approx \left(3 + \frac{T_b^\circ}{T_u}\right)\frac{\lambda_u}{\rho_u S_u^\circ c_p} \qquad (A34)$$

and

$$\frac{\hat{m_C}}{A} \approx 3.3\,\frac{g_u \lambda_u}{S_u^\circ c_p} \qquad (A35)$$

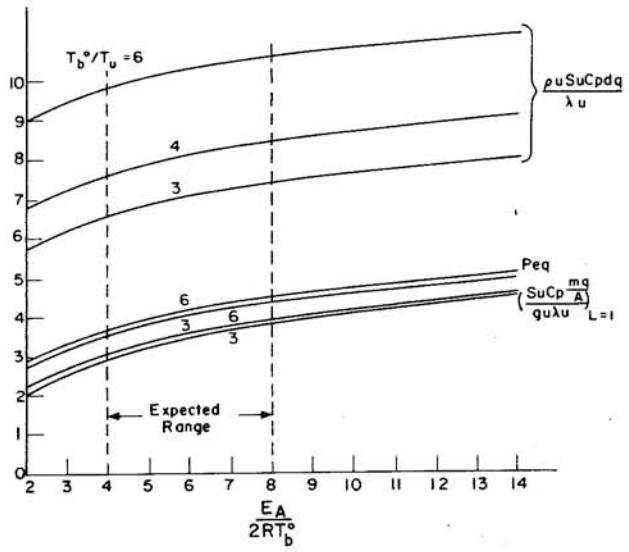

Fig. A1 - Parametric solutions to Laminar Flame Quenching Equation

APPENDIX REFERENCES

A1 C. R. Ferguson, "Stand-Off Distance on a Flat Flame Burner," Combustion and Flame, 34, 1979.

A2 D. B. Spalding, Combustion and Flame, 1, 296 (1957).

A3 W. T. Kaskan, Sixth Symposium (International) on Combustion, Baltimore: Williams and Wilkins, Baltimore 1953 p. 126.

LIST OF SYMBOLS

f_{CR} - Mole fraction of HC in Reservoir (ppmC)

f_{CB} - Mole fraction of HC in Bomb (ppmC)

N_C - Number of moles of unburned carbon after combustion

N_B - Total moles of gas in Bomb before sampling

N_R - Total moles of gas in Reservoir before sampling

P_R - Final pressure of system after diluting with N_2.

V_B - Bomb volume

V_R - Reservoir volume

T_B - Bomb wall temperature

T_R - Reservoir wall temperature

R - Universal gas constant

N_b - Number of moles of products in Bomb after combustion

W_u - Molecular weight for unburned gases

W_b - Molecular weight for burned gases

N_u - Number of moles of initial unburned mixture in Bomb

P_i - Initial pressure

f_C - Mole fraction of carbon in the Bomb products

$[N_C]$ - Bomb HC concentration after combustion

$[N_u]$ - Initial unburned charge concentration

V_o - Molar volume at STP

T_o - Standard Temperature (273 K)

P_o - Standard Pressure (1 atm)

ϕ - Equivalence Ratio

f_I - Mass fraction of inert gas diluent

N_{Cc} - Number of HC moles stored in crevice following combustion

V_c - Volume of crevice

P_p - Peak pressure

f_{Cu} - Mole fraction of carbon in initial mixture

$[N_{Cc}]$ - Bomb HC concentrations produced by fuel stored in crevices

$[N_{Cnc}]$ - Bomb HC concentrations produced by non-crevice sources

m_C - Mass of carbon determined experimentally

A_B - Bomb interior wall area (cm^2)

W_C - Molecular weight of carbon

m_{Cq} - Mass of carbon at moment of quenching proposed by Ferguson and Keck [10]

λ_u - Thermal conductivity

g_{Cu} - Mass fraction of carbon in the unburned mixture

S_u° - Adiabatic burning velocity

C_p - Average specific heat at constant pressure

Society of Automotive Engineers, Inc.
400 COMMONWEALTH DRIVE, WARRENDALE, PA 15096

16 page booklet.

Printed in U.S.A.